frontiers | Frontiers in Mechanical Engineering

REVIEW
published: 25 May 2022
doi: 10.3389/fmech.2022.910415

Mechanics and Strategies for Wrinkling Suppression: A Review

Zhaojie Zhang[1†], *Lingyu Zhao*[2†] *and Jidong Shi*[1*]

[1]College of Engineering Physics, Shenzhen Technology University, Shenzhen, China, [2]Department of Materials Science and Engineering, Southern University of Science and Technology, Shenzhen, China

Wrinkling is a well-known phenomenon observed at various length scales for diverse materials. Despite a variety of research studies focusing on investigating wrinkling mechanisms and utilizing them to create surface patterns recently, wrinkling also brings about the loss of specific functional properties that were initially endowed to the thin films. For instance, wrinkling may result in the degradation of electrical and optical properties of the film; and the wrinkled films are easily delaminated. Therefore, it is still meaningful to find ways for the suppression of wrinkling on the thin film, although the relevant works are far less than those that utilize the surface instability to achieve certain structures. In this review, the approaches to restrain the emergence of wrinkles will be introduced. Following the introduction part, numerical analysis for wrinkle generation will be first discussed, by which the key parameters determining wrinkle initiation and morphology will be provided. Then, wrinkle suppression strategies by tailoring these parameters will be introduced in the following sections. This review aims to provide useful guidance for future research on alleviating surface fluctuations and achieving desired device functionality.

Keywords: wrinkles, thin films, coatings, compressive stress, flexible electronics

OPEN ACCESS

Edited by:
Liu Wang,
Massachusetts Institute of Technology, United States

Reviewed by:
Guorui Wang,
University of Science and Technology of China, China
Yifan Rao,
The University of Texas at Austin, United States

****Correspondence:***
Jidong Shi
shijidong@sztu.edu.cn

†These authors have contributed equally to this work and share the first authorship

Specialty section:
This article was submitted to Solid and Structural Mechanics, a section of the journal Frontiers in Mechanical Engineering

Received: *01 April 2022*
Accepted: *22 April 2022*
Published: *25 May 2022*

Citation:
Zhang Z, Zhao L and Shi J (2022) Mechanics and Strategies for Wrinkling Suppression: A Review. Front. Mech. Eng 8:910415. doi: 10.3389/fmech.2022.910415

INTRODUCTION

Rugged surfaces are ubiquitous in nature, with feature sizes spanning from kilometer scale for mountain ranges to the micro- and nanometer scale for biological membranes, such as animal skins, brain cortex, and leaf laminae. Usually, surface fluctuations and patterns could be generated through biological self-assembly, selective etching, and the out-of-plane bending, taking advantage of surface instabilities (Rodriguez-Hernandez, 2015). In recent years, the artificial design of surface fluctuations has been widely applied for enhanced cell adhesion (Chen et al., 2011), stretchable electronics (Kim et al., 2010) (Dai et al., 2021), and the construction of smart surfaces (Hou et al., 2019) (Zhao et al., 2018). Compared with the bottom-up approach such as self-assembly and microfabrication, which is laborious and time-consuming, the top–down approach by transforming global compressive strain into surface wrinkles is facile with low cost and has drawn increasing attention nowadays. Since the morphology of surface wrinkles could be customized by predefining the material type and structure of the system and adjusting the value and orientation of the compressive strain, dramatic theoretical and experimental efforts have been devoted to developing programable surface patterns with fine control (Xue et al., 2020).

A wrinkled surface could be spontaneously generated within a suspended ultrathin film, such as graphene, to reduce the total Gibbs-free energy (Meyer et al., 2007). More commonly, surface wrinkles emerge within a bilayer system, with a film laminated on an underlying substrate. The biological wrinkles, such as wrinkles on the skin and fruit exocarp, are caused by mechanical mismatch between the external layer (dermis or exocarp) and the inner layer (hypodermis or

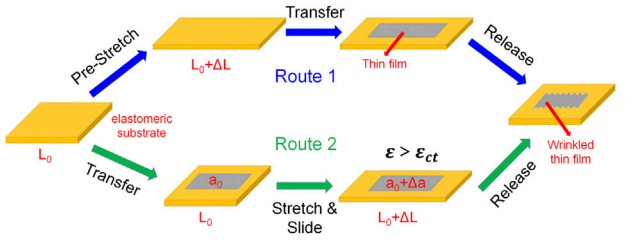

FIGURE 1 | Schematics of the two routes for wrinkle generation within a bilayer system.

sarcocarp) as a result of certain chemical and biological processes (Fujimura et al., 2007) (Dai et al., 2014). For wrinkles in the synthetic bilayer system, the mechanical mismatch is mostly created by applied strain on the substrate. There are two general routes for wrinkle generation in the bilayer system (**Figure 1**). First, the substrate is prestretched before the deposition/coating of the top-layer film. Upon the release of the prestrain, the film is synchronously compressed by the interfacial shear stress and develops wrinkles for energy minimization (Kaltenbrunner et al., 2013). Second, for a bilayer system without initial strain, the applied tensile strain of the substrate cannot be completely transferred to the top-layer film, endowing an interfacial sliding. Upon strain release, the strain mismatch leads to a compression of the film by which surface wrinkles are generated (Jiang et al., 2014) (Lipomi et al., 2011). Wrinkles generated by uniaxial compression usually demonstrate wavelike structure, with a certain wavelength and amplitude, which are also called buckles. If the compressive strain is multiaxial or omnidirectional, the resulting wrinkle morphology could be regarded as the superposition of uniaxial buckles, which is complex with low directivity. The formation of a wrinkled structure endows stretchability to an intrinsically brittle film by accommodating the tensile strain through the flattening of wrinkles, which is significant in the design of flexible electronics (Rogers et al., 2010) (Kim et al., 2020).Moreover, the buckled surface could also be applied as optical gratings (Hu et al., 2020) and self-cleaning coatings (Pocivavsek et al., 2019), showing great potential in the design of smart devices.

Despite the versatile applications of surface wrinkles, in many scenarios, the emergence of wrinkles is undesirable. For example, wrinkles on human skin are considered a sign of the aging process, and wrinkles on fruit exocarp indicate the loss of freshness. Moreover, the generation of surface wrinkles could cause the reduction of optical transparency, abrasion resistance, and electronic carrier mobility, which further lead to degradation and even failure of materials and devices (Kim et al., 2016). For example, wrinkles on CVD-derived graphene greatly increase the scattering and reduce the quantum localization of charge carriers by which the charge carrier mobility is greatly reduced (Zhu et al., 2012) (Deng and Berry, 2016). To this end, it is of great significance to seek strategies for the restraint of surface wrinkles. However, the relevant study is far less than utilizing surface instabilities for wrinkle generation, and the mechanism for wrinkling suppression is seldom discussed.

In this review, the approaches for the suppression of surface wrinkles will be introduced. In **Section 2**, the numerical analysis of the wrinkle generation process in a two-layer system will be given, with the emphasis on the key parameters determining the initiation of wrinkles and the wrinkle amplitude and wavelength. In **Sections 3–5**, three different strategies for restraining wrinkles in a two-layer system will be provided, including the control of film–substrate interactions and the stiffness and thickness of the top-layer film. This review will be ended by a discussion of the challenges and prospects for further development of wrinkle suppression strategies.

NUMERICAL ANALYSIS OF WRINKLE GENERATION

Since the first analytical study on the out-of-plane bending of a compressed column in Euler's work in the 18th century (Landau et al., 1986), the wrinkling theory has been developing continuously with transdisciplinary research, combining mechanics and materials science. In brief, wrinkling of a certain subject initiates when compressive stress reaches a critical value and further the in-plane compression is not energetically favorable compared to the out-of-plane bending. In recent years, wrinkling within a bilayer system, with a film supported on an underlying substrate, has drawn increasing attention due to its easy implementation and significant application in flexible electronics. As discussed in the previous section, the driving force for film wrinkling is the compressive load by the interfacial shear stress and could be mathematically described by several key parameters, including the strain/load needed for wrinkle initiation and the wavelength and amplitude of the wrinkles. These parameters could be mathematically calculated through the minimization of the total energy, including the elastic energy of both the substrate and the film and the bending energy of the film. Notably, the discussion is based on the prerequisite that there is no interfacial delamination and sliding so that the interfacial energy remains the same before and after wrinkling. (Song, 2015) (Hu et al., 2019), In the case of uniaxial compression, the three types of energy of the film could be described by the following equations:

Elastic energy of the film:

$$U_f = \frac{1}{2}\bar{E}_f t_f \left(\frac{\pi^2 A^2}{\lambda^2} - \varepsilon_{com}\right)^2 L_0, \tag{1}$$

Elastic energy of the substrate:

$$U_s = \frac{\pi}{4\lambda}\bar{E}_s A^2 L_0, \tag{2}$$

Bending energy of the film:

$$U_b = \frac{\pi^4 \bar{E}_f t_f^3 A^2}{3\lambda^4} L_0, \tag{3}$$

Energy in total:

$$U_\Sigma = U_f + U_s + U_b, \tag{4}$$

where $\bar{E}_f$ and $\bar{E}_s$ are the plane-strain moduli of the film and substrate, respectively, which are determined by their corresponding elastic modulus (E_f and E_s) and Poisson's ratio (μ_f and μ_s) as $\bar{E}_f = \frac{E_f}{1-\mu_f^2}$ and $\bar{E}_s = \frac{E_s}{1-\mu_s^2}$; t_f is the thickness of the film; A and λ are the amplitude and wavelength of the wrinkles, respectively; ε_{com} is the total compressive strain applied by the substrate to the film, which could be the prestrain in the prestretch-release scenario or the mismatch strain in the stretch-slide scenario; L_0 is the length of the film. The thermodynamic stability of the system necessitates the minimization of U_Σ, indicating:

$$\frac{\partial U_\Sigma}{\partial A} = \frac{\partial U_\Sigma}{\partial \lambda} = 0, \tag{5}$$

The λ and A could be resolved from **Eqs. 1–5** as follows:

$$\lambda = 2\pi t_f \left(\frac{\bar{E}_f}{3\bar{E}_s}\right)^{\frac{1}{3}}, \tag{6}$$

$$A = t_f \sqrt{\frac{4\varepsilon_{com}\left(\bar{E}_f\right)^{\frac{2}{3}}}{\left(3\bar{E}_s\right)^{\frac{2}{3}}}}, \tag{7}$$

On the other hand, the wrinkling behavior of a substrate-supported thin film could also be analyzed by a force balance equation (Chung et al., 2011):

$$F = 4\bar{E}_f I\left(\frac{\pi}{\lambda}\right)^2 + \frac{\bar{E}_s w}{4}\left(\frac{\pi}{\lambda}\right)^{-1}, \tag{8}$$

where F is the shear load on the film when wrinkles initiate; I is the moment of inertia, defined as $I = \frac{wt_f^3}{12}$; w is the width of the film. By substituting the expression of λ in **Eq. 6** into **Eq. 8**, the expression of F could be written as follows:

$$F = \frac{\sqrt[3]{9}}{4} t_f w\left(\bar{E}_f\right)^{\frac{1}{3}}\left(\bar{E}_s\right)^{\frac{2}{3}}, \tag{9}$$

The corresponding critical shear stress (τ_c) and strain (ε_c) could be derived from **Eq. 9**, which are expressed as follows:

$$\tau_c = \frac{\sqrt[3]{9}}{4}\left(\bar{E}_f\right)^{\frac{1}{3}}\left(\bar{E}_s\right)^{\frac{2}{3}}. \tag{10}$$

$$\varepsilon_c = \frac{1}{4}\left(\frac{3\bar{E}_s}{\bar{E}_f}\right)^{\frac{2}{3}}. \tag{11}$$

By combining **Eq. 7** and **Eq. 11** the expression of A could be simplified as follows:

$$A = t_f \sqrt{\frac{\varepsilon_{com}}{\varepsilon_c} - 1}. \tag{12}$$

For wrinkles generated in the prestretch-release scenario, the parameters A, λ, and ε_c are sufficient to describe the emergence and property of wrinkles, which are determined by the moduli of both the substrate and the film, the thickness of the film, and the prestrain, while for wrinkles generated in the stretch–slide scenario, the critical strain for interfacial sliding (ε_s) should also be noticed, which could be calculated by the shear-lag model (Jiang et al., 2014) as follows:

$$\varepsilon_s = \frac{\tau_m}{\sqrt{\bar{E}_s \bar{E}_f}} coth\left(\frac{L_0}{2}\sqrt{\frac{\bar{E}_s}{\bar{E}_f}}\right), \tag{13}$$

where τ_m is the maximum shear stress for a certain bilayer interface, which is determined by the bonding manner and strength between layers. For wrinkle emergence in a stretch–slide manner, the critical initial tensile strain (ε_{ct}) should equal the sum of ε_s and ε_c, written as follows:

$$\varepsilon_{ct} = \varepsilon_s + \varepsilon_c = \frac{1}{4}\left(\frac{3\bar{E}_s}{\bar{E}_f}\right)^{\frac{2}{3}} + \frac{\tau_m}{\sqrt{\bar{E}_s \bar{E}_f}} coth\left(\frac{L_0}{2}\sqrt{\frac{\bar{E}_s}{\bar{E}_f}}\right), \tag{14}$$

With regard to the suppression of wrinkles, the stretch–slide mode should be taken into prioritized consideration since the prestretch-release mode is usually applied to actively prepare wrinkles. Thereafter, the ε_{ct} value should be tailored large enough to avoid wrinkling caused by unexpected strain (e.g., thermal expansion, solution swelling . . .). From **Eq. 14**, ε_{ct} increases with τ_m, which indicates that enhancing the interfacial interactions could be a strategy for wrinkle suppression by the reduced tendency of interfacial sliding and strain mismatch. On the other hand, all numerical discussion in this section is based on the prerequisite that no delamination between the film and substrate occurs. While it no longer stands when the interfacial shear stress is too low, the resulted delaminated wrinkles and folds could be greatly detrimental to the surface flatness. Therefore, the strong interfacial adhesion is significant in both scenarios for wrinkle suppression. **Eq. 14** also implies that ε_{ct} increases with the reduction of $\bar{E}_f$. On the other hand, when $\bar{E}_f$ is very high, which makes τ_c higher than τ_m, the shear stress is insufficient to initiate the out-of-plane deformation of the film. Thus, wrinkling could also be avoided. Based on the aforementioned discussion, the modulus of the film plays a complicated role in wrinkle initiation, and wrinkle suppression through film modulus control could be achieved through two opposite methodologies by designing either ultracompliant or ultrastiff films. Moreover, when wrinkles have already been generated, minimization of wrinkle amplitude could also be regarded as "wrinkle suppression" by reducing surface roughness, which could be achieved by decreasing the film thickness t according to **Eq. 12**. Notably, from **Eq. 11**, reduction of substrate modulus also favors the suppression of wrinkles, while in practice, it is seldom applied because of the low cost-effectiveness and deteriorated overall flexibility of the bilayer system.

In the following section, the approaches for suppressing surface wrinkles will be introduced according to the aforementioned parameters. In **Section 3**, the strategies for enhancing the interfacial strength between the film and substrate will be introduced. In **Section 4**, the modulus control of the film for wrinkle restraint will be discussed, including the introduction of porosity within the film to

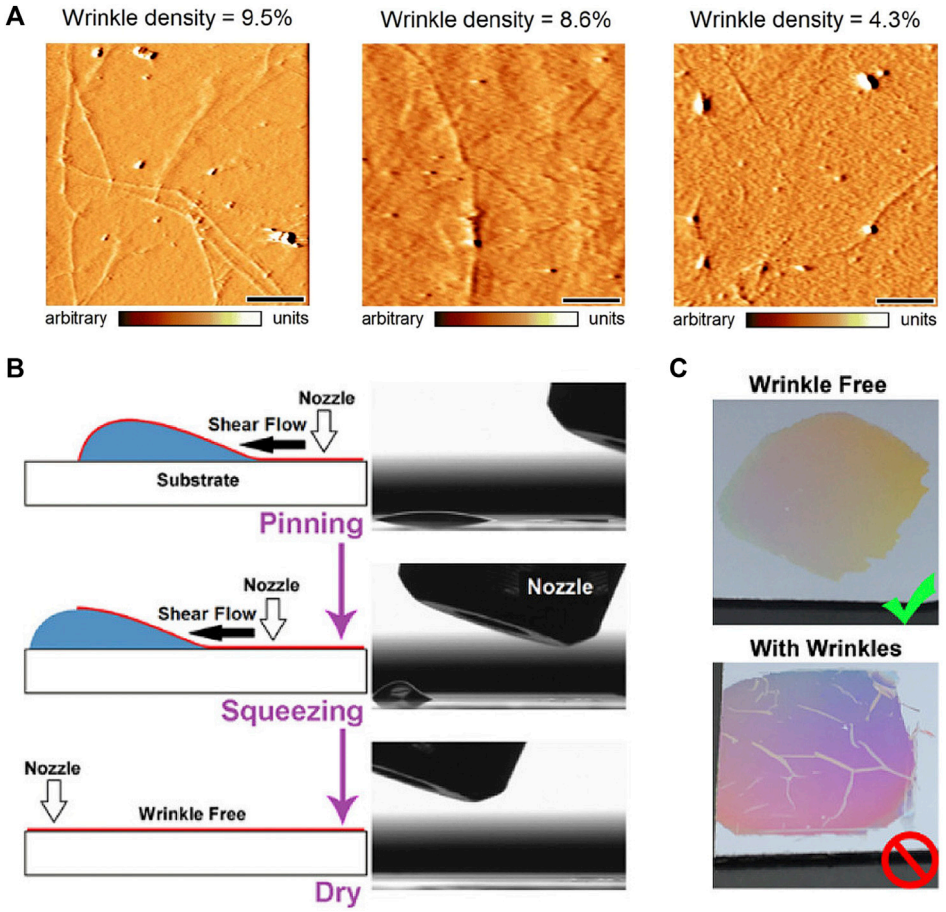

FIGURE 2 | Wrinkle suppression through modulation of the bilayer interface. **(A)** Wrinkle density of the graphene film on substrates with different roughness. The substrates from left to right are flat SiO_2, flat HfO_2, and rough HfO_2, with increased initial surface roughness from left to right. Also, the resulted wrinkle density decreases from left to right. Scale bar: 1.5 μm (reproduced with permission from Lanza et al., 2013, the American Institute of Physics). **(B)** Schematic (left) and corresponding optical image (right) of directional airflow–assisted wet transfer of anodic aluminum oxide (AAO) film. **(C)** The wrinkle-free film by flow-assisted wet transfer (top) and wrinkled film by normal wet transfer (bottom) (reproduced with permission from Zhang et al., 2021, The American Chemical Society).

mitigate lateral Poisson wrinkling, and reinforcement of the film rigidity to prevent compression induced wrinkling. In **Section 5**, the reduction of wrinkle amplitude through thickness control of the film will be introduced.

WRINKLE SUPPRESSION THROUGH INTERFACE MODULATION

As discussed in the last section, strong bonding between the film and underlying substrate could mitigate interfacial sliding in a bilayer system, and wrinkles are avoided through a synchronized deformation of the two layers (Wang et al., 2016) (Wang G. et al., 2021). The general ways to improve the interfacial bonding strength are as follows: 1. increasing the contact area between layers through patterning. A rough surface of the substrate could be obtained by replicating a natural/artificial template with micro/nanoscale patterns. The meandering paths among the surface render a much higher surface area than a smooth one, which could be inherited by the film after a conformal transfer or deposition (Liu et al., 2017) (Shi et al., 2018). 2. Improving the interlayer adhesion through chemical modification at the interface. Normally, the bonding between the film and substrate is the van der Waals attraction, which is long-range and weak. The introduction of certain functional groups on the substrate facilitates stronger interfacial interactions, such as covalent bonding, donor–acceptor (D–A) interactions, and hydrogen bonding. 3. The intermediate layer could be introduced to improve the adhesion strength. 4. Removal of contaminants at the interface.

Strategies for Wrinkle Suppression by Improving the Interlayer Strength

A scalable way to increase the contact area between layers lies in a bio-inspired design at the contact interface. Since the biological surfaces, such as leaf, flower, and animal skin, usually have a hierarchical structure with micro- and nanoscale patterns, many researchers take advantage of the patterns by casting the polymer

precursors on the biological template. After curing and peeling off from the template, a polymer substrate with a bio-templated surface is prepared, and a thin film could be deposited or transferred to the patterned substrate surface to finish the bilayer preparation. Inspired by skin electronics utilizing the surface roughness of skins to increase the bio-electronics conformity, the enlarged interfacial area through templated patterning also improves the adhesion between the synthetic bilayer (Liu et al., 2022). The as-prepared bilayer structure could be applied for wide-range pressure sensing and stretchable electronics (Wei et al., 2015) (Shi et al., 2019) and utilized in the suppression of wrinkles. Lanza et al. investigated the wrinkling behavior of graphene film on both flat and rough substrates. The rough surface dramatically improves the adhesion of graphene on the substrate by which the density and amplitude of wrinkles are greatly reduced (**Figure 2A**) (Lanza et al., 2013). Wang et al. discussed the effects of feature size and shape of the surface asperities on the conformity of graphene adhesion and the resulted wrinkle morphology using molecular dynamics (MD) simulation. Substrate surfaces with mild perturbations and valleys are more favorable in film adhesion and wrinkle suppression than surfaces with sharper ones (Wang et al., 2018). Using a rough surface for wrinkle suppression also has some drawbacks. First, the surface roughness brings about the difficulty of the conformal transfer of the film to the substrate, with an increased tendency for gap generation. Moreover, stress concentration could be induced by the patterns at the bilayer interface, which leads to crack generation among the film. On the other hand, surface patterns could be intrinsically detrimental to the properties and performance of the bi-layer structure, just as the negative effect on the formation of wrinkles. In addition, when a film is transferred on a substrate with high-aspect-ratio patterns, undesired delaminated wrinkles, such as tents, could be generated because conformal interfacial contact is not energetically favorable (Dai and Lu, 2021). As a result, the price for wrinkle suppression may not be acceptable in practical scenarios.

The introduction of strong interlayer bondings also leads to a dramatically improved adhesion force. A simple way to achieve this goal is through a hydrophilic treatment of the substrate, including UV illumination, O_2 plasma cleaning, and treatment with strong oxidant, before deposition of the film (Efimenko et al., 2005) (Bodas and Khan-Malek, 2006). The hydrophilic treatment could usually generates an oxygen-rich layer on the polymer surface, which facilitates the adhesion of the top-layer film in the wet transfer process or film deposition by solution coating. Moreover, a polymer-assisted metal deposition strategy, which is an intermediate layer with strong interactions with both the substrate and the film, is introduced at the bilayer interface, and a dramatically improved stress transfer could be achieved (Yu et al., 2014) (Li P. et al., 2019) (Rhee et al., 2019). By grafting a self-assembled 3-mercaptopropyltrimethoxysilane (MPTMS) layer on the PDMS substrate, the deposited Au film could be tightly anchored to the substrate by the strong Au–S covalent bond. The resulted bilayer is scratch-resistant and wrinkle-free even after the release of a 100% prestrain (Guo et al., 2016). Li et al. deposited a poly (methacrylic acid) (PMAAc) layer on the PDMS surface before a PEDOT-PSS film is deposited. The methyl groups in pristine PDMS are substituted by carboxyl groups, which dramatically enhance the adhesion of the PEDOT-PSS layer through hydrogen bonding (Li G. et al., 2019). Increased interfacial adhesion by the ionic bond and coordination bond has also been reported (Wang et al., 2011; Wang et al., 2013). Moreover, a spatially controlled wrinkling of the graphene film could be achieved through chemical modification at specific regions, by which wrinkles only form in the weakly bonded unmodified area (Hallam et al., 2015) (Li et al., 2020).

Strategies to Eliminate Wrinkles Within CVD-Derived 2D Materials

2D materials, such as graphene and transition metal dichalcogenides (TMDs), could be prepared in a large area through chemical vapor deposition (CVD) (Cai et al., 2018). Despite significant applications in electronic and optoelectronic devices, the electronic and optical properties of 2D membranes could be deteriorated with wrinkles generated during the growth and transfer process. During the cooling process after the high-temperature CVD growth, the mismatch of the thermal expansion coefficient (CTE) between 2D materials and metal substrates causes an unsynchronized deformation, and the residual stress from the substrate could trigger the wrinkle formation of 2D membranes (Zhu et al., 2012) (Deng and Berry, 2016). Tremendous efforts have been devoted to minimizing this detrimental wrinkling. Except for the selection of the catalytic substrate with similar CTE to the resulted 2D membranes (Lee et al., 2014) and the reduction of growth temperature for less strain mismatch (Wang M. et al., 2021), which are susceptible to degrade the film quality, a milder approach lies in the modification of the graphene–substrate interface. Valerius et al. irradiated the iridium (Ir) substrate with 500 eV He + plasma before the CVD growth of graphene. The intercalated He + ion dramatically increases the delamination energy between graphene and the Ir substrate, and graphene wrinkles could be prevented (Valerius et al., 2019). Mun et al. improved the conformity between the Cu foil substrate and CVD-derived graphene through a preliminary hot pressing of the substrate. The resulted graphene demonstrates a smooth morphology with a minimized batch-to-batch difference in carrier transport properties (Mun et al., 2015). On the other hand, in the wet transfer process of the CVD-derived 2D materials to the targeted substrate, droplets are spontaneously trapped at the membrane-substrate interface for the minimization of elastic energy of the membrane, the van der Waals interaction–related interfacial energy, and the surface tension–related energy of the droplet (Sanchez et al., 2018) (Rao et al., 2021). After the evaporation of droplets, wrinkles form due to the confinement of droplet fringes. To tackle this issue, a directional airflow (**Figures 2B,C**), or the introduction of organic liquid with low surface tension could promote a quick removal of the droplets and facilitate a smooth lamination of the membrane and substrates (Zhang et al., 2021) (Kim et al., 2016) (Liu et al., 2019). Deposition of a titanium layer onto the target substrate facilitates a wrinkle-free transfer of graphene through strong Ti-O-C chemical bonding, while the conductive Ti layer

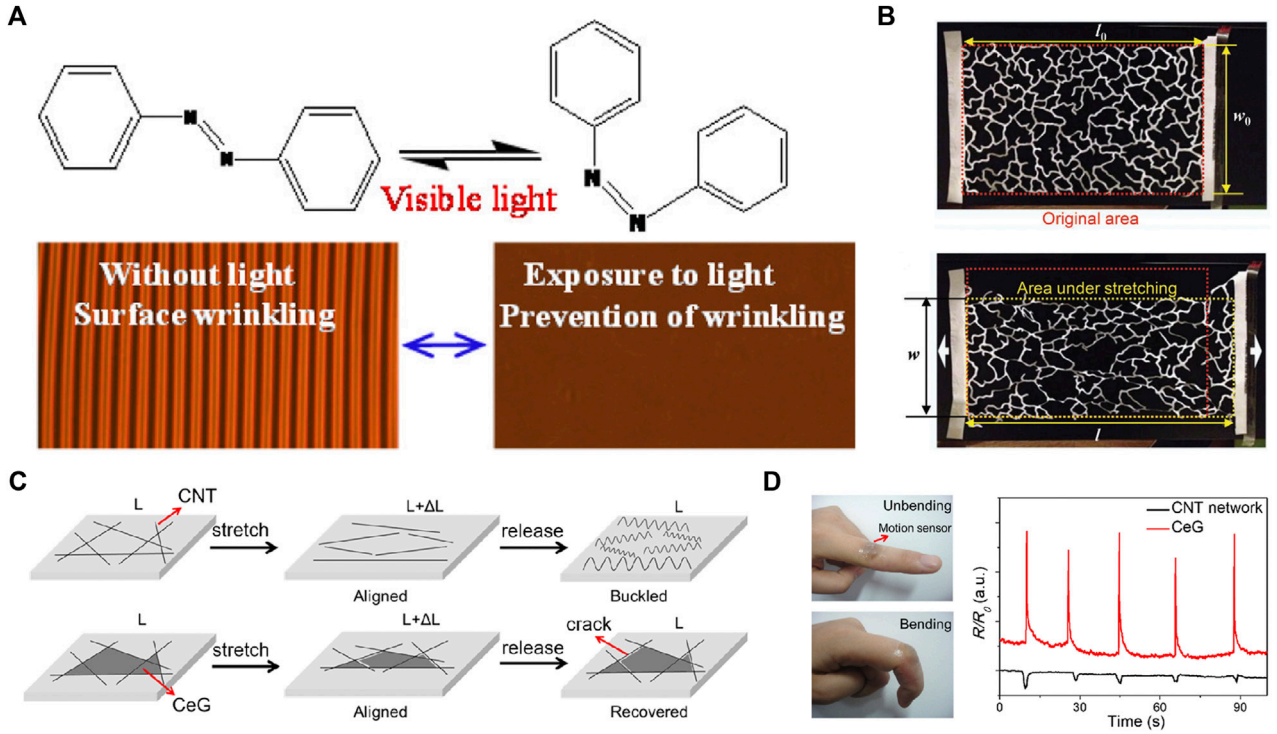

FIGURE 3 | Wrinkle suppression through film stiffness modulation. **(A)** Mechanism of the photoisomerization process of the PAAB film (top) and the reversible light-triggered de-wrinkling (bottom) (reproduced with permission from Ji et al., 2016, The American Chemical Society). **(B)** Unstretched (top) and stretched (bottom) AuNM-PDMS electrode, with lateral Poisson's wrinkles suppressed with large tensile strain (reproduced with permission from Wang et al., 2019, Wiley-VCH). **(C)** Mechanism of buckle suppression of the CNT film through graphene hybridization. **(D)** Comparison between a CeG-based strain sensor and a CNT-based strain sensor in detecting a strain by finger bending (reproduced with permission from Shi et al., 2016, Wiley-VCH).

restricts the application of the transferred film (Lee et al., 2017) (Park et al., 2015).

WRINKLE SUPPRESSION THROUGH FILM STIFFNESS CONTROL

According to the discussion in **Section 2**, the film stiffness in the bilayer system could dramatically influence the formation and morphology of wrinkles. For the suppression of wrinkles, the film could be designed to be either ultracompliant, by which the interfacial shear stress could be adapted by the in-plane deformation instead of the out-of-plane bending, or ultrastiff, by which the interfacial shear stress is insufficient to initiate the wrinkling. Both ideas have been applied in practical wrinkle suppression. To this end, the stiffness modulation strategies could be divided into two categories, which will be discussed in this section.

Compliance Improvement to Increase Wrinkling Threshold

From **Eq. 11**, the critical strain for wrinkling increases with the compliance of the film in the bilayer system. Ji et al. developed a bilayer system with photo-responsive poly (p-aminoazobenzene) (PAAB) film supported by the PDMS substrate. Upon visible light illumination, a photoisomerization process of the PAAB film is initiated, by which the modulus decreases dramatically by its change in configuration. The initial wrinkling caused by the transfer process could be facilely eliminated by the photoisomerization process through a light-triggered spontaneous stress release (**Figure 3A**). (Ji et al., 2016) However, the application of the strategy by chemically modifying a continuous film is limited. Compliance improvement is more commonly achieved by a topological design of the film, which will be introduced in this part.

The optimization of human–machine interfacing necessitates improved flexibility and stretchability of electronic devices. Despite versatile strategies to achieve stretchability, the tensile stretch in the axial direction is usually accompanied by a lateral contraction due to the ubiquitous Poisson effect, by which wrinkles could be unavoidably generated. The Poisson wrinkles could be detrimental to the performance of flexible devices, by deteriorated electrical properties, increased optical haze, and reduced durability caused by interfacial delamination (Drack et al., 2015) (Yunusa et al., 2018). The basic idea to tackle this issue is to make the in-plane deformation more mechanically and energetically favorable than the out-of-plane wrinkling.

While the compressive stiffness and bending stiffness usually varies synchronously for a continuous film, it is difficult to minimize Poisson's wrinkling by mere material selection. To this end, the topological design of the film is adopted as an efficient strategy to suppress lateral Poisson's wrinkles.

Through numerical simulation, Yan et al. claimed that Poisson's wrinkles could be restrained by perforation near the center of the film within the bilayer system, through the modification of the local stress field, and the effect could be influenced by the position, radius, shape and spatial distribution of the holes (Yan et al., 2014). Furthermore, research using molecular dynamics (MD) modulation by the same group validated that introduction of rigid elements near the lateral edges of the stretched film also favors the suppression of lateral Poisson's wrinkles (Yan et al., 2016). Li, Luo, and collaborators simulated the stress distribution of polymer-supported rigid films with versatile topologies using finite element (FE) and MD modeling and supposed optimized surface topologies for wrinkle suppression. These results provided useful guidance in the design of flexible electronics (Li et al., 2017) (Luo et al., 2017).

Epidermal electronics, which could be seamlessly adhered to human skin, show significant promise in health monitoring due to the efficient signal transduction between the human body and electronic device (Kim et al., 2011) (Chung et al., 2019). However, the ultrahigh stretchability of human skin could bring about not only cracks in the axial direction but also wrinkles and even delamination due to the lateral Poisson compression, which greatly deteriorates the reliability and durability of sensing. In order to mitigate lateral Poisson's wrinkle in epidermal electronic devices, Wang et al. developed a gold nanomesh-poly (dimethylsiloxane) (AuNM-PDMS) electrode with ultrahigh mechanical compliance, which could be tightly adhered to human skin. With a mesoporous kirigami structure, the AuNM-PDMS film demonstrates a wrinkle-free surface even with a compressive strain of 100% owing to its superior capability for the in-plane deformation (Figure 3B). The AuNM-PDMS film could be used as the electrode of a capacitive sensor and demonstrates stable performance during 1,000 stretching–releasing cycles with 100% strain (Wang et al., 2019).

Stiffness Reinforcement for Wrinkle Suppression

According to **Eqs 11** and **12**, the increase of film modulus within the bilayer system leads to lower critical strain and higher wrinkling amplitude, which is unfavorable for wrinkle suppression. Nevertheless, the critical wrinkling stress $\boldsymbol{\tau_c}$ also increases with film modulus (**Eq. 10**). When $\boldsymbol{\tau_c}$ becomes higher than maximum shear stress $\boldsymbol{\tau_m}$, wrinkling of the film can no longer be initiated. To this end, reinforcement of film stiffness could be an effective approach in wrinkle prevention.

For the strengthening of mechanically compliant polymers, the strategy of embedding rigid particulates into the polymer matrix is widely applied. Hendricks and Lee reinforced a PDMS-supported polyelectrolyte multilayer film by incorporating silica nanoparticles within it. Wrinkles generated by cyclic thermal stress could be efficiently mitigated after the addition of nanoparticles, with surface roughness decreased by three orders compared with a wrinkled film without reinforcement (Hendricks and Lee, 2007). Birman also validated the effect through the addition of stiff nanoinclusions to an epoxy film on buckle prevention through a numerical analysis. The reinforcement effects could be lost when the compressive stress is so high by which an interface failure between the nanoinclusions and matrix could be generated (Birman, 2019).

The membrane comprising randomly overlapped carbon nanotubes (CNTs) is highly conductive and flexible and could maintain some electrical conductivity even with a 200% tensile strain, which is highly suitable for wide-range strain sensing. However, upon the release of strain, the CNT membrane develops wave-like buckles, leading to deteriorated sensitivity and reliability in cyclic strain sensing. Shi et al. tackled this issue by an *in situ* CVD growth of graphene among the nanoporous CNT template. The resulted CNT-decorated graphene (CeG) demonstrated a leaf-like structure, with CNT and graphene seamlessly hybridized; the periodic buckles of the CNT film under cyclic stretch are prevented (**Figure 3C**). Moreover, the CeG film demonstrated a monotonic and linear electromechanical response within 20% strain, rather than a minor resistance peak around 0% strain for the pristine CNT film, which shows greatly improved reliability in recording small strains (**Figure 3D**). (Shi et al., 2016) They further optimized the CeG structure by substituting the random CNT film with the cross-stacked CNT film, with two aligned CNT arrays stacked in the orthogonal direction. The cross-stacked CNT-graphene hybrid demonstrates anti-wrinkling behavior along both aligned directions, with strain sensitivity increased by 5–10 times due to increased interlayer stress transfer (Shi et al., 2017).

DECREASE OF FILM THICKNESS FOR REDUCED WRINKLE AMPLITUDE

According to **Eqs 6**, **11**, and **12**, the onset strain for wrinkle formation does not rely on film thickness, while the amplitude and wavelength of wrinkles are proportional to the film thickness. Therefore, it is a facile strategy to control the wrinkle morphology by tailoring the thickness of the film within a bilayer structure, which can be further applied in building smart surfaces (Li et al., 2013) (Zhao et al., 2018). For mitigation of surface roughness caused by wrinkling, a film with limited thickness is favorable. For the heterogeneous bilayer system, it is feasible to control the film thickness by tuning the operating parameters in the deposition or coating process. On the other hand, the exposure of polymeric elastomers to environmental hazards, such as ozone and UV radiation, could trigger the oxidation on the elastomer's surface, and a stiff surface layer could be generated (Efimenko et al., 2005). Upon manual or

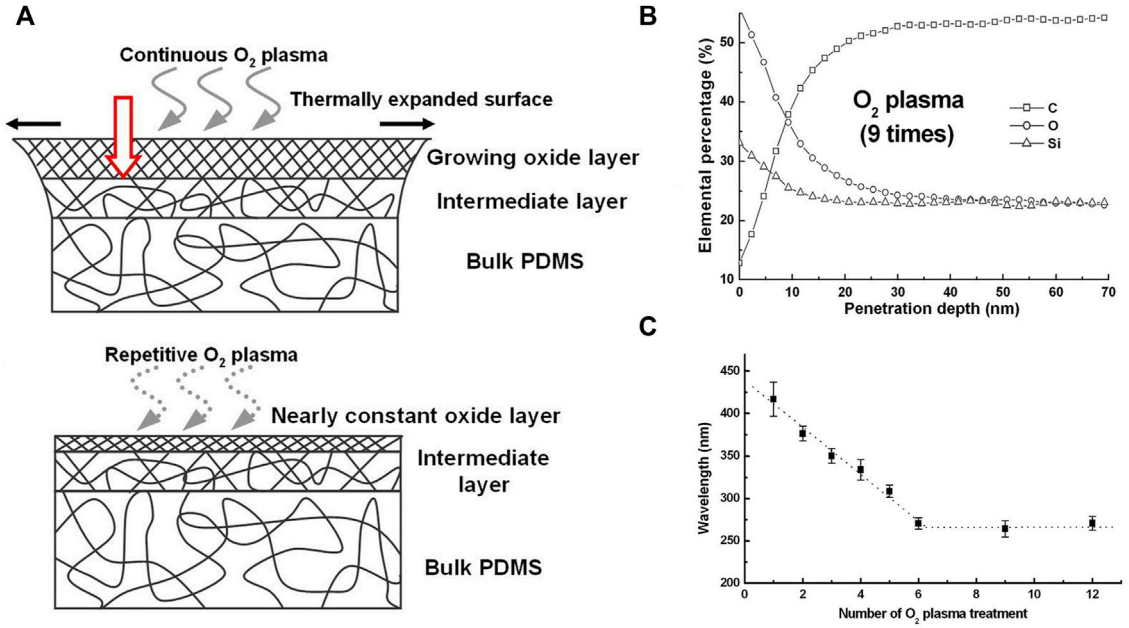

FIGURE 4 | Wrinkle suppression through film thickness control. **(A)** Schematics of the comparison between the development of the surface oxide layer by continuous and intermittent O_2 plasma treatment. **(B)** Elemental distribution of C, O, and Si with depth, indicating the formation of a SiO_2-based rigid oxide layer. **(C)** Wavelength of the generated wrinkles with the number of intermittent O_2 plasma treatments. The wavelength becomes stable after six cycles of treatment, indicating that the thickness of the rigid layer no longer increases (reproduced with permission from Park et al., 2010, The Royal Society of Chemistry).

environmental strain of the elastomer, wrinkles emerge on the rigid top layer, which could cause a deteriorated performance of the polymer. In the following discussion, the ways to control the thickness of the oxidation layer in polymeric elastomers will be introduced.

The oxidization layer on the elastomer is generated by the exposure of the elastomer to radiation and hazardous chemicals. From the engineering level, surface oxidation could be mitigated by decreasing exposure time and radiation intensity/hazard concentration. Moreover, the introduction of protection layers could also slow down the emergence and development of the oxidation layer (Cooper et al., 2008). For elastomers utilized in the oxidative environment for the long term, Park et al. raised two approaches to limit the thickness of the oxidation layer. The first approach is through a combinative treatment of UV/ozone and oxygen plasma, which could generate a viscoelastic intermediate layer between the rigid oxidation layer and matrix. In addition, compared with continuous exposure to the oxidative source, by which the thickness of the oxidation layer increases monotonically with time, intermittent treatment with O_2 plasma for a short period of time (eg:1 min) could generate a rigid oxidation layer with finite thickness (**Figure 4**), which serves as an effective barrier layer for the further penetration of reactive species. Therefore, the depth of the oxidation layer will no longer expand with further exposure to the oxidative source. Although the rigidity increase also contributes to the increase of wrinkle amplitude, its influence (power number: $\frac{1}{3}$) is much lower than the decrease in thickness (power number: 1) from **Eq. 7** (Park et al., 2010).

CONCLUSION AND PROSPECTS

Although wrinkling is no longer regarded as detrimental in materials science, there is still great motivation in developing efficient wrinkle suppression strategies for optimized performance of electronic and optical devices. To this end, the strategies for wrinkle suppression in various scenarios are introduced in this review in order to provide some helpful guidance in this field. From the numerical analysis of wrinkle generation and development, we picked up key parameters determining the threshold for wrinkle initiation and the morphology of resulting wrinkles. To increase the critical strain for wrinkling, the interface property and stiffness of the thin film within the bilayer system could be tailored. Moreover, the reduction of wrinkle amplitude could also be regarded as wrinkle suppression, which could be achieved through the decrease of film thickness. Through various material modification and structural design methodologies, the aforementioned parameters could be facilely tuned, and improved anti-wrinkling performances are achieved.

Further development of anti-wrinkling strategies lies in the balance between wrinkle suppression performance and maintenance of the intrinsic functionalities in a specific system since the suppression of wrinkles is always at the expense of some degradation of other properties. For example, the stiffness reinforcement of films usually leads to reduced stretchability and optical transparency, and

modification of the interface between the metal film and elastomer could decrease the electrical conductivity of the film. Moreover, surface patterning could induce the formation of folds and delaminated wrinkles and the inhomogeneous stress distribution which leads to stress concentration and cracking. The state-of-the-art anti-wrinkling strategies should be comprehensively evaluated before being adopted in a certain system and further optimization of the strategies that minimize the side effect to the intrinsic material properties is still waiting to be carried out. Sustained and coordinated efforts from mechanics, materials science, and mechanical engineering should be further devoted in this field to address this challenge and eventually achieve optimized anti-wrinkling performance.

AUTHOR CONTRIBUTIONS

ZZ and JS developed the idea, and ZZ and JS conducted the literature research. ZZ, LZ, and JS wrote the manuscript, and LZ and JS reviewed and revised the manuscript.

FUNDING

JS thanks the support from the National Natural Science Foundation of China (22109104) and the Youth Innovation Talent Project of Guangdong Education Department (2021KQNCX081); LZ thanks the support from the National Natural Science Foundation of China (52103301). JS thanks Natural Science Foundation of top talent of SZTU (grant number: GDRC202101).

REFERENCES

Birman, V. (2019). Enhancing Toughness of Thin Films and Coatings through Embedded Nanoinclusions. *Z. Angew. Math. Mech.* 99 (1), e201800159. doi:10.1002/zamm.201800159

Bodas, D., and Khan-Malek, C. (2006). Formation of More Stable Hydrophilic Surfaces of PDMS by Plasma and Chemical Treatments. *Microelectron. Eng.* 83 (4-9), 1277–1279. doi:10.1016/j.mee.2006.01.195

Cai, Z., Liu, B., Zou, X., and Cheng, H.-M. (2018). Chemical Vapor Deposition Growth and Applications of Two-Dimensional Materials and Their Heterostructures. *Chem. Rev.* 118 (13), 6091–6133. doi:10.1021/acs.chemrev.7b00536

Chen, A., Lieu, D. K., Freschauf, L., Lew, V., Sharma, H., Wang, J., et al. (2011). Shrink-Film Configurable Multiscale Wrinkles for Functional Alignment of Human Embryonic Stem Cells and Their Cardiac Derivatives. *Adv. Mat.* 23 (48), 5785–5791. doi:10.1002/adma.201103463

Chung, H. U., Kim, B. H., Lee, J. Y., Lee, J., Xie, Z., Ibler, E. M., et al. (2019). Binodal, Wireless Epidermal Electronic Systems with In-Sensor Analytics for Neonatal Intensive Care. *Science* 363 (6430), eaau0780. doi:10.1126/science.aau0780

Chung, J. Y., Nolte, A. J., and Stafford, C. M. (2011). Surface Wrinkling: A Versatile Platform for Measuring Thin-Film Properties. *Adv. Mat.* 23 (3), 349–368. doi:10.1002/adma.201001759

Cooper, R., Upadhyaya, H. P., Minton, T. K., Berman, M. R., Du, X., and George, S. M. (2008). Protection of Polymer from Atomic-Oxygen Erosion Using Al2O3 Atomic Layer Deposition Coatings. *Thin Solid Films* 516 (12), 4036–4039. doi:10.1016/j.tsf.2007.07.150

Dai, H.-H., and Liu, Y. (2014). Critical Thickness Ratio for Buckled and Wrinkled Fruits and Vegetables. *EPL* 108 (4), 44003. doi:10.1209/0295-5075/108/44003

Dai, Y., Hu, H., Wang, M., Xu, J., and Wang, S. (2021). Stretchable Transistors and Functional Circuits for Human-Integrated Electronics. *Nat. Electron.* 4 (1), 17–29. doi:10.1038/s41928-020-00513-5

Dai, Z., and Lu, N. (2021). Poking and Bulging of Suspended Thin Sheets: Slippage, Instabilities, and Metrology. *J. Mech. Phys. Solids* 149, 104320. doi:10.1016/j.jmps.2021.104320

Deng, S., and Berry, V. (2016). Wrinkled, Rippled and Crumpled Graphene: an Overview of Formation Mechanism, Electronic Properties, and Applications. *Mater. Today* 19 (4), 197–212. doi:10.1016/j.mattod.2015.10.002

Drack, M., Graz, I., Sekitani, T., Someya, T., Kaltenbrunner, M., and Bauer, S. (2015). An Imperceptible Plastic Electronic Wrap. *Adv. Mat.* 27 (1), 34–40. doi:10.1002/adma.201403093

Efimenko, K., Rackaitis, M., Manias, E., Vaziri, A., Mahadevan, L., and Genzer, J. (2005). Nested Self-Similar Wrinkling Patterns in Skins. *Nat. Mater* 4 (4), 293–297. doi:10.1038/nmat1342

Fujimura, T., Haketa, K., Hotta, M., and Kitahara, T. (2007). Loss of Skin Elasticity Precedes to Rapid Increase of Wrinkle Levels. *J. Dermatological Sci.* 47 (3), 233–239. doi:10.1016/j.jdermsci.2007.05.002

Guo, C. F., Chen, Y., Tang, L., Wang, F., and Ren, Z. (2016). Enhancing the Scratch Resistance by Introducing Chemical Bonding in Highly Stretchable and Transparent Electrodes. *Nano Lett.* 16 (1), 594–600. doi:10.1021/acs.nanolett.5b04290

Hallam, T., Shakouri, A., Poliani, E., Rooney, A. P., Ivanov, I., Potie, A., et al. (2015). Controlled Folding of Graphene: GraFold Printing. *Nano Lett.* 15 (2), 857–863. doi:10.1021/nl503460p

Hendricks, T. R., and Lee, I. (2007). Wrinkle-free Nanomechanical Film: Control and Prevention of Polymer Film Buckling. *Nano Lett.* 7 (2), 372–379. doi:10.1021/nl062544q

Hou, H., Yin, J., and Jiang, X. (2019). Smart Patterned Surface with Dynamic Wrinkles. *Acc. Chem. Res.* 52 (4), 1025–1035. doi:10.1021/acs.accounts.8b00623

Hu, K. M., Liu, Y. Q., Zhou, L. W., Xue, Z. Y., Peng, B., Yan, H., et al. (2020). Delamination-Free Functional Graphene Surface by Multiscale, Conformal Wrinkling. *Adv. Funct. Mater.* 30 (34), 2003273. doi:10.1002/adfm.202003273

Hu, X., Dou, Y., Li, J., and Liu, Z. (2019). Buckled Structures: Fabrication and Applications in Wearable Electronics. *Small* 15 (32), 1804805. doi:10.1002/smll.201804805

Ji, H., Zhao, Y., Zong, C., Xie, J., Han, X., Wang, J., et al. (2016). Simple and Versatile Strategy to Prevent Surface Wrinkling by Visible Light Irradiation. *ACS Appl. Mat. Interfaces* 8 (29), 19127–19134. doi:10.1021/acsami.6b04868

Jiang, T., Huang, R., and Zhu, Y. (2014). Interfacial Sliding and Buckling of Monolayer Graphene on a Stretchable Substrate. *Adv. Funct. Mat.* 24 (3), 396–402. doi:10.1002/adfm.201301999

Kaltenbrunner, M., Sekitani, T., Reeder, J., Yokota, T., Kuribara, K., Tokuhara, T., et al. (2013). An Ultra-lightweight Design for Imperceptible Plastic Electronics. *Nature* 499 (7459), 458–463. doi:10.1038/nature12314

Kim, D.-H., Lu, N., Ma, R., Kim, Y.-S., Kim, R.-H., Wang, S., et al. (2011). Epidermal Electronics. *Science* 333 (6044), 838–843. doi:10.1126/science.1206157

Kim, D.-H., Xiao, J., Song, J., Huang, Y., and Rogers, J. A. (2010). Stretchable, Curvilinear Electronics Based on Inorganic Materials. *Adv. Mat.* 22 (19), 2108–2124. doi:10.1002/adma.200902927

Kim, D. C., Shim, H. J., Lee, W., Koo, J. H., and Kim, D. H. (2020). Material-Based Approaches for the Fabrication of Stretchable Electronics. *Adv. Mat.* 32 (15), 1902743. doi:10.1002/adma.201902743

Kim, H. H., Lee, S. K., Lee, S. G., Lee, E., and Cho, K. (2016). Wetting-Assisted Crack- and Wrinkle-free Transfer of Wafer-Scale Graphene onto Arbitrary Substrates over a Wide Range of Surface Energies. *Adv. Funct. Mat.* 26 (13), 2070–2077. doi:10.1002/adfm.201504551

Landau, L. D., Lifshitz, E. M., Kosevich, A. d. M., and Pitaevskii, L. P. (1986). *Theory of Elasticity: Volume 7*. Amsterdam, Netherlands: Elsevier.

Lanza, M., Wang, Y., Bayerl, A., Gao, T., Porti, M., Nafria, M., et al. (2013). Tuning Graphene Morphology by Substrate towards Wrinkle-free Devices: Experiment and Simulation. *J. Appl. Phys.* 113 (10), 104301. doi:10.1063/1.4794521

Lee, J.-H., Lee, E. K., Joo, W.-J., Jang, Y., Kim, B.-S., Lim, J. Y., et al. (2014). Wafer-scale Growth of Single-Crystal Monolayer Graphene on Reusable Hydrogen-Terminated Germanium. *Science* 344 (6181), 286–289. doi:10.1126/science.1252268

Lee, S.-H., Kim, J.-H., Park, B.-J., Park, J., Kim, H.-S., and Yoon, S.-G. (2017). Wrinkle-free Graphene Electrodes in Zinc Tin Oxide Thin-Film Transistors for Large Area Applications. *Nanotechnology* 28 (7), 075205. doi:10.1088/1361-6528/aa55e6

Li, G., Qiu, Z., Wang, Y., Hong, Y., Wan, Y., Zhang, J., et al. (2019a). PEDOT:PSS/Grafted-PDMS Electrodes for Fully Organic and Intrinsically Stretchable Skin-like Electronics. *ACS Appl. Mat. Interfaces* 11 (10), 10373–10379. doi:10.1021/acsami.8b20255

Li, M., Niu, Y., Wu, H., Zhang, X., Luo, Y., and Kang, Z. (2017). Wrinkling and Wrinkling-Suppression in Graphene Membranes with Frozen Zone. *Thin Solid Films* 638, 345–353. doi:10.1016/j.tsf.2017.08.009

Li, P., Zhang, Y., and Zheng, Z. (2019b). Polymer-Assisted Metal Deposition (PAMD) for Flexible and Wearable Electronics: Principle, Materials, Printing, and Devices. *Adv. Mat.* 31 (37), 1902987. doi:10.1002/adma.201902987

Li, T., Hu, K., Ma, X., Zhang, W., Yin, J., and Jiang, X. (2020). Hierarchical 3D Patterns with Dynamic Wrinkles Produced by a Photocontrolled Diels-Alder Reaction on the Surface. *Adv. Mat.* 32 (7), 1906712. doi:10.1002/adma.201906712

Li, Y., Dai, S., John, J., and Carter, K. R. (2013). Superhydrophobic Surfaces from Hierarchically Structured Wrinkled Polymers. *ACS Appl. Mat. Interfaces* 5 (21), 11066–11073. doi:10.1021/am403209r

Lipomi, D. J., Vosgueritchian, M., Tee, B. C.-K., Hellstrom, S. L., Lee, J. A., Fox, C. H., et al. (2011). Skin-like Pressure and Strain Sensors Based on Transparent Elastic Films of Carbon Nanotubes. *Nat. Nanotech* 6 (12), 788–792. doi:10.1038/nnano.2011.184

Liu, S., Rao, Y., Jang, H., Tan, P., and Lu, N. (2022). Strategies for Body-Conformable Electronics. *Matter* 5 (4), 1104–1136. doi:10.1016/j.matt.2022.02.006

Liu, X., Huang, K., Zhao, M., Li, F., and Liu, H. (2019). A Modified Wrinkle-free MoS2 Film Transfer Method for Large Area High Mobility Field-Effect Transistor. *Nanotechnology* 31 (5), 055707. doi:10.1088/1361-6528/ab49b8

Liu, Z., Wang, X., Qi, D., Xu, C., Yu, J., Liu, Y., et al. (2017). High-Adhesion Stretchable Electrodes Based on Nanopile Interlocking. *Adv. Mat.* 29 (2), 1603382. doi:10.1002/adma.201603382

Luo, Y., Xing, J., Niu, Y., Li, M., and Kang, Z. (2017). Wrinkle-free Design of Thin Membrane Structures Using Stress-Based Topology Optimization. *J. Mech. Phys. Solids* 102, 277–293. doi:10.1016/j.jmps.2017.02.003

Meyer, J. C., Geim, A. K., Katsnelson, M. I., Novoselov, K. S., Booth, T. J., and Roth, S. (2007). The Structure of Suspended Graphene Sheets. *Nature* 446 (7131), 60–63. doi:10.1038/nature05545

Mun, J. H., Oh, J. G., Bong, J. H., Xu, H., Loh, K. P., and Cho, B. J. (2015). Wrinkle-free Graphene with Spatially Uniform Electrical Properties Grown on Hot-Pressed Copper. *Nano Res.* 8 (4), 1075–1080. doi:10.1007/s12274-014-0585-x

Park, B. J., Choi, J. S., Kim, H. S., Kim, H. Y., Jeong, J. R., Choi, H. J., et al. (2015). Realization of Large-Area Wrinkle-free Monolayer Graphene Films Transferred to Functional Substrates. *Sci. Rep.* 5 (1), 9610–9617. doi:10.1038/srep09610

Park, J.-Y., Chae, H. Y., Chung, C.-H., Sim, S. J., Park, J., Lee, H. H., et al. (2010). Controlled Wavelength Reduction in Surface Wrinkling of Poly(dimethylsiloxane). *Soft Matter* 6 (3), 677–684. doi:10.1039/b916603c

Pocivavsek, L., Ye, S.-H., Pugar, J., Tzeng, E., Cerda, E., Velankar, S., et al. (2019). Active Wrinkles to Drive Self-Cleaning: A Strategy for Anti-thrombotic Surfaces for Vascular Grafts. *Biomaterials* 192, 226–234. doi:10.1016/j.biomaterials.2018.11.005

Rao, Y., Qiao, S., Dai, Z., and Lu, N. (2021). Elastic Wetting: Substrate-Supported Droplets Confined by Soft Elastic Membranes. *J. Mech. Phys. Solids* 151, 104399. doi:10.1016/j.jmps.2021.104399

Rhee, D., Paci, J. T., Deng, S., Lee, W.-K., Schatz, G. C., and Odom, T. W. (2019). Soft Skin Layers Enable Area-specific, Multiscale Graphene Wrinkles with Switchable Orientations. *ACS Nano* 14 (1), 166–174. doi:10.1021/acsnano.9b06325

Rodríguez-Hernández, J. (2015). Wrinkled Interfaces: Taking Advantage of Surface Instabilities to Pattern Polymer Surfaces. *Prog. Polym. Sci.* 42, 1–41. doi:10.1016/j.progpolymsci.2014.07.008

Rogers, J. A., Someya, T., and Huang, Y. (2010). Materials and Mechanics for Stretchable Electronics. *Science* 327 (5973), 1603–1607. doi:10.1126/science.1182383

Sanchez, D. A., Dai, Z., Wang, P., Cantu-Chavez, A., Brennan, C. J., Huang, R., et al. (2018). Mechanics of Spontaneously Formed Nanoblisters Trapped by Transferred 2D Crystals. *Proc. Natl. Acad. Sci. U.S.A.* 115 (31), 7884–7889. doi:10.1073/pnas.1801551115

Shi, J., Hu, J., Dai, Z., Zhao, W., Liu, P., Zhao, L., et al. (2017). Graphene Welded Carbon Nanotube Crossbars for Biaxial Strain Sensors. *Carbon* 123, 786–793. doi:10.1016/j.carbon.2017.08.006

Shi, J., Li, X., Cheng, H., Liu, Z., Zhao, L., Yang, T., et al. (2016). Graphene Reinforced Carbon Nanotube Networks for Wearable Strain Sensors. *Adv. Funct. Mat.* 26 (13), 2078–2084. doi:10.1002/adfm.201504804

Shi, J., Lv, S., Wang, L., Dai, Z., Yang, S., Zhao, L., et al. (2019). Crack Control in Biotemplated Gold Films for Wide-Range, Highly Sensitive Strain Sensing. *Adv. Mat. Interfaces* 6 (20), 1901223. doi:10.1002/admi.201901223

Shi, J., Wang, L., Dai, Z., Zhao, L., Du, M., Li, H., et al. (2018). Multiscale Hierarchical Design of a Flexible Piezoresistive Pressure Sensor with High Sensitivity and Wide Linearity Range. *Small* 14 (27), 1800819. doi:10.1002/smll.201800819

Song, J. (2015). Mechanics of Stretchable Electronics. *Curr. Opin. Solid State Mater. Sci.* 19 (3), 160–170. doi:10.1016/j.cossms.2015.01.004

Valerius, P., Herman, A., and Michely, T. (2019). Suppression of Wrinkle Formation in Graphene on Ir(111) by High-Temperature, Low-Energy Ion Irradiation. *Nanotechnology* 30 (8), 085304. doi:10.1088/1361-6528/aaf534

Wang, G., Dai, Z., Liu, L., Hu, H., Dai, Q., and Zhang, Z. (2016). Tuning the Interfacial Mechanical Behaviors of Monolayer Graphene/PMMA Nanocomposites. *ACS Appl. Mat. Interfaces* 8 (34), 22554–22562. doi:10.1021/acsami.6b03069

Wang, G., Liu, L., and Zhang, Z. (2021). Interface Mechanics in Carbon Nanomaterials-Based Nanocomposites. *Compos. Part A Appl. Sci. Manuf.* 141, 106212. doi:10.1016/j.compositesa.2020.106212

Wang, M., Huang, M., Luo, D., Li, Y., Choe, M., Seong, W. K., et al. (2021). Single-crystal, Large-Area, Fold-free Monolayer Graphene. *Nature* 596 (7873), 519–524. doi:10.1038/s41586-021-03753-3

Wang, S., Ma, Y., Pan, F., Shao, L., and Chen, Y. (2018). A Mode-independent Energy Method in Morphology Prediction of Graphene on Substrates with Nanoscale Asperities. *Int. J. Mech. Sci.* 146-147, 355–365. doi:10.1016/j.ijmecsci.2018.08.001

Wang, X., Hu, H., Shen, Y., Zhou, X., and Zheng, Z. (2011). Stretchable Conductors with Ultrahigh Tensile Strain and Stable Metallic Conductance Enabled by Prestrained Polyelectrolyte Nanoplatforms. *Adv. Mat.* 23 (27), 3090–3094. doi:10.1002/adma.201101120

Wang, X., Zhang, T., Kobe, B., Lau, W. M., and Yang, J. (2013). Grafting of Polyelectrolytes onto Hydrocarbon Surfaces by High-Energy Hydrogen Induced Cross-Linking for Making Metallized Polymer Films. *Chem. Commun.* 49 (41), 4658–4660. doi:10.1039/c3cc41644e

Wang, Y., Liu, Q., Zhang, J., Hong, T., Sun, W., Tang, L., et al. (2019). Giant Poisson's Effect for Wrinkle-Free Stretchable Transparent Electrodes. *Adv. Mat.* 31 (35), 1902955. doi:10.1002/adma.201902955

Wei, Y., Chen, S., Lin, Y., Yang, Z., and Liu, L. (2015). Cu-Ag Core-Shell Nanowires for Electronic Skin with a Petal Molded Microstructure. *J. Mat. Chem. C* 3 (37), 9594–9602. doi:10.1039/c5tc01723h

Xue, Z., Song, H., Rogers, J. A., Zhang, Y., and Huang, Y. (2020). Mechanically-Guided Structural Designs in Stretchable Inorganic Electronics. *Adv. Mat.* 32 (15), 1902254. doi:10.1002/adma.201902254

Yan, D., Huangfu, D., Zhang, K., and Hu, G. (2016). Wrinkling of the Membrane with Square Rigid Elements. *EPL* 116 (2), 24005. doi:10.1209/0295-5075/116/24005

Yan, D., Zhang, K., Peng, F., and Hu, G. (2014). Tailoring the Wrinkle Pattern of a Microstructured Membrane. *Appl. Phys. Lett.* 105 (7), 071905. doi:10.1063/1.4893596

Yu, Y., Yan, C., and Zheng, Z. (2014). Polymer-Assisted Metal Deposition (PAMD): A Full-Solution Strategy for Flexible, Stretchable, Compressible, and Wearable Metal Conductors. *Adv. Mat.* 26 (31), 5508–5516. doi:10.1002/adma.201305558

Yunusa, M., Amador, G. J., Drotlef, D.-M., and Sitti, M. (2018). Wrinkling Instability and Adhesion of a Highly Bendable Gallium Oxide Nanofilm Encapsulating a Liquid-Gallium Droplet. *Nano Lett.* 18 (4), 2498–2504. doi:10.1021/acs.nanolett.8b00164

Zhang, H., Zhou, M., Guo, Y., Yu, Z., Xu, R., Wen, L., et al. (2021). Gas-Flow-Assisted Wrinkle-free Transfer of a Centimeter-Scale Ultrathin Alumina

Membrane onto Arbitrary Substrates. *ACS Appl. Mat. Interfaces* 13 (29), 35124–35132. doi:10.1021/acsami.1c07574

Zhao, L., Zhang, L., Zhao, J., Shi, J., Dai, Z., Wang, G., et al. (2018). Engineering Surface Patterns with Shape Memory Polymers: Multiple Design Dimensions for Diverse and Hierarchical Structures. *ACS Appl. Mat. Interfaces* 11 (1), 1563–1570. doi:10.1021/acsami.8b15535

Zhu, W., Low, T., Perebeinos, V., Bol, A. A., Zhu, Y., Yan, H., et al. (2012). Structure and Electronic Transport in Graphene Wrinkles. *Nano Lett.* 12 (7), 3431–3436. doi:10.1021/nl300563h

Conflict of Interest: The authors declare that the research was conducted in the absence of any commercial or financial relationships that could be construed as a potential conflict of interest.

Publisher's Note: All claims expressed in this article are solely those of the authors and do not necessarily represent those of their affiliated organizations, or those of the publisher, the editors, and the reviewers. Any product that may be evaluated in this article, or claim that may be made by its manufacturer, is not guaranteed or endorsed by the publisher.